

# DIRECT THRUST MEASUREMENT OF THE ENPULSION NANO R<sup>3</sup> PROPULSION SYSTEM ON FOTEC'S THRUST TEST STAND

Presented at the 8<sup>th</sup> Space Propulsion Conference  
Estoril, Portugal / 9 – 13 May 2022

**Bernhard Seifert** <sup>(1)</sup>, **Werner Engel** <sup>(2)</sup>, **Joachim Gerger** <sup>(3)</sup>  
FOTEC Forschungs- und Technologietransfer GmbH

<sup>(1)</sup> *Head of Aerospace Engineering Department, seifert@fotec.at*

<sup>(2)</sup> *Senior Scientist, engel@fotec.at*

<sup>(3)</sup> *Scientist, gerger@fotec.at*

**Quirin Koch** <sup>(4)</sup>, **Tony Schönherr** <sup>(5)</sup>, **David Krejci** <sup>(6)</sup>  
ENPULSION GmbH

<sup>(4)</sup> *Product Manager, quirin.koch@enpulsion.com*

<sup>(5)</sup> *Product Manager NANO, tony.schoenherr@enpulsion.com*

<sup>(6)</sup> *CTO, krejci@enpulsion.com*

**KEYWORDS:** FEEP, IFM, electric propulsion, ion thruster, ion emitter, LMIS, micro-propulsion system, propulsion module, direct thrust measurement

## ABSTRACT

In 2021 FOTEC performed a direct thrust measurement campaign of the ENPULSION NANO R<sup>3</sup> micro-propulsion system. In recent years FOTEC has developed their thrust test stand suitable for measurements from the sub- $\mu\text{N}$  up to 100 mN range without modification of the setup. The force actuators providing force-feedback and a test force were calibrated before the test campaign. The ENPULSION NANO R<sup>3</sup> with integrated PPU was mounted on the thrust balance and supplied via liquid-metal based feedthroughs. After burn-in, different thrust points and profiles were applied by digitally commanding the propulsion system like in a spacecraft. The thruster parameters and the thrust balance telemetry were recorded, and the thrust values were compared to the mathematical model. To minimize any chamber-induced effects, FOTEC's largest vacuum facility (ca. 14 m<sup>3</sup>) was used for this campaign. This paper shows the test setup and presents the results acquired within this campaign.

## 1 INTRODUCTION

The ENPULSION NANO R<sup>3</sup> is a fully integrated propulsion system including propellant tank and power electronics to achieve the required high voltages and control thereof, providing 350  $\mu\text{N}$  at variable specific impulse and a maximum power draw of 45 W [1]. It is based on the IFM Nano Thruster – now ENPULSION NANO – developed by FOTEC and in-orbit demonstrated in 2018. The thruster gained significant flight heritage since then as more than 80 thrusters are in space today. The thrust is generated by electrostatically extracting and accelerating indium ions from Taylor cones which form on the needle tips of a porous, crown-shaped emitter [2]. The firmware uses the underlying mathematical model to compute the thrust and specific impulse and incorporates two dependent PID controllers to match the reference values provided [3].

FOTEC developed a torsion-based thrust balance with frictionless spring bearings and high precision active force feedback. With different ranges, the balance can operate from the sub- $\mu\text{N}$  range up to the 1 N range [4], [5]. Low-friction liquid-metal based electric high-voltage high-current feedthroughs, ultra-flexible gas supply and a contactless cooling

system allow the operation of different electric propulsion systems without compromising measurement accuracy or drift rate. A previous generation of the used horizontal torsion balance was successfully qualified at ESTEC in 2014 [6]. For different operation points the thrust was computed by the firmware using internal telemetry and compared with direct thrust measurements.

## 2 FEEP TECHNOLOGY

For over two decades, FOTEC has developed the mN-FEEP (Field Emission Electric Propulsion) thruster to be used in future science missions [7]. This thruster can provide highly accurate thrust ranging from 1  $\mu\text{N}$  to above 1 mN [8]. It allows large satellites to control their position and orientation with an unprecedented accuracy [9]. In order to emit ions a so-called crown emitter (see Figure 1) is being used, that has been developed by FOTEC for the upcoming Earth observation mission NGGM (Next Generation Gravity Mission) [10]–[13].

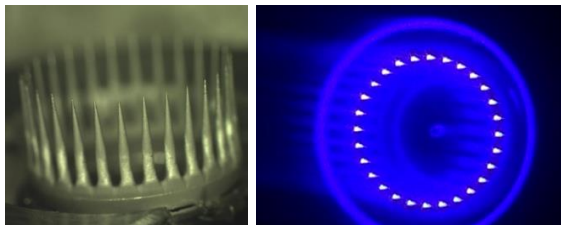


Figure 1. The porous crown emitter (left) and in operation at the FOTEC laboratories (right)

An endurance test of a 28-needle emitter is currently ongoing and has so far reached more than 41,000 hours of firing time in a dedicated vacuum facility. This demonstrates that FOTEC’s proprietary FEEP technology is suitable for long-term scientific and Earth observation missions with high reliability and high total impulse requirements.

## 3 THE ENPULSION NANO R<sup>3</sup> THRUSTER

In order to use the crown emitters as part of an integrated propulsion system for nanosatellites, the entire thruster was optimized in terms of mass and volume. In parallel, a PPU (Power Processing Unit) was developed and integrated into the thruster module – the IFM Nano Thruster (Indium FEEP Multiemitter) [14], [15].

In early 2018, a 3U CubeSat equipped with such an IFM Nano Thruster module was launched with the PSLV-C40 from India. For the first time, a FEEP based propulsion system could be operated in-orbit and two successful orbit raise maneuvers could be performed [16].

Based on the heritage NANO thruster and increased requirements for the electronics, a family of improved propulsion systems featuring higher radiation-tolerant electronics was developed. Figure 2 shows the NANO R<sup>3</sup> propulsion module.



Figure 2. The ENPULSION NANO R<sup>3</sup> integrated propulsion system

Like the IFM Nano Thruster, the NANO R<sup>3</sup> consists of a single crown emitter, two redundant thermionic neutralizers and an integrated PPU. In contrast, the electronic components of the NANO R<sup>3</sup> PPU are more resilient against TID (Total Ionizing Dose) and SEE (Single Event Effects). The key features of the micro-propulsion system are listed in Table 1.

Dynamic thrust range	10 to 350 $\mu\text{N}$
Nominal thrust	350 $\mu\text{N}$
Specific impulse	2,000 to 6,000 s
Propellant mass	220 g
Total impulse	> 5,000 Ns
Power (nom. thrust)	45 W (incl. neutralizer)
Dimensions	98.0 x 99.0 x 95.3 mm
Mass dry / wet	< 1,180 g / < 1,400 g
Total system power	10 to 45 W
Hot standby power	5 W
Command interface	RS-422 / RS-485
Temperature (storage)	-40 to +95 °C
Temperature (operational)	-20 to +40 °C
Supply voltage	12 V or 28 V

Table 1. Key features of the NANO R<sup>3</sup> micro-propulsion system [17]

#### 4 THE FOTEC $\mu\text{N}$ TO $\text{mN}$ THRUST BALANCE

In recent years, FOTEC developed several generations of  $\mu\text{N}$  test stands [18], [19], [5]. Though significant improvements concerning the thrust noise, stability and response time could be achieved, the basic operation principle was not changed. Such a thrust balance consists of a horizontal torsion pendulum suspended by two spring bearings. The thruster or propulsion module is mounted on one side of the beam and counterweights are placed on the other side (see Figure 3).

Up to eight liquid-metal based electric feedthroughs, rated for up to 20 kV / 3 A are located in the axis of rotation. These supply the DUT (Device Under Test) without compromising the thrust measurement accuracy compared to the use of thin wire leads.

If required for HETs (Hall Effect Thrusters) or GITs (Gridded Ion Thrusters), low-tension flexible tubes for gaseous propellant supply can be installed.

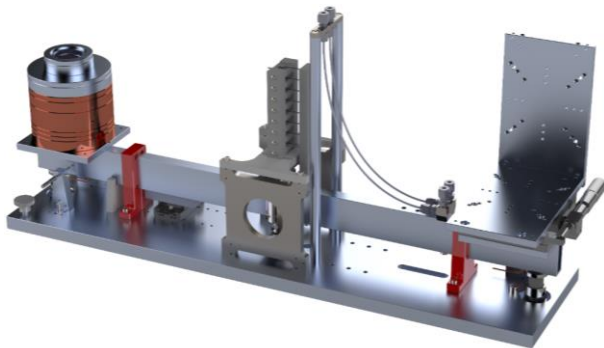


Figure 3. FOTEC's horizontal torsion-based thrust balance

When the thruster is operated, the beam starts to move, and its deflection is measured by an optical displacement sensor based on relative reflectivity. Electro-magnetic force actuators (so-called "voice coils") are used to pull back the beam to resting position. This is achieved by a software-based closed-loop PID controller. Due to the force-feedback operation mode, the response time of the system can be reduced, and the voice coils are always operated in proper alignment. An additional damping system is not required. A second force actuator, located underneath the thruster, is used to apply a test force which allows the in-situ verification of the entire system. The key features and limitations of the thrust balance are listed in Table 2.

Compatible thrusters	Electric, cold gas
Thruster mass / footprint	< 15 kg / < 200 x 200 mm
Thrust range	< 1 $\mu\text{N}$ to 1 N
Noise floor	< 0.15 $\mu\text{N}_{\text{RMS}}$ at 500 $\mu\text{N}$
Long-term stability	< 2 $\mu\text{N}/\text{h}$ at 500 $\mu\text{N}$
Accuracy	< 2%, see [5] for details
Electric feedthroughs	8x, 20 kV / 3 A
Propellant feedthroughs	2x, gas
Operation mode	Force feedback
Force actuators	2x, electro-magnetic

Table 2. Key features of FOTEC's  $\mu\text{N}$  to  $\text{mN}$  thrust balance

#### 5 TEST SETUP

The test campaign was conducted in FOTEC's largest vacuum facility with a volume of ca. 14  $\text{m}^3$ . This ensures minimal chamber effects usually caused by gaseous backflow or backscattered ions. The NANO R<sup>3</sup> was mounted on the thrust balance using a dedicated adapter (see Figure 4, right bottom). Supply, enclosure grounding and digital communication lines (RS-422) of the module were fed through the liquid metal contacts (see Figure 4, left bottom).

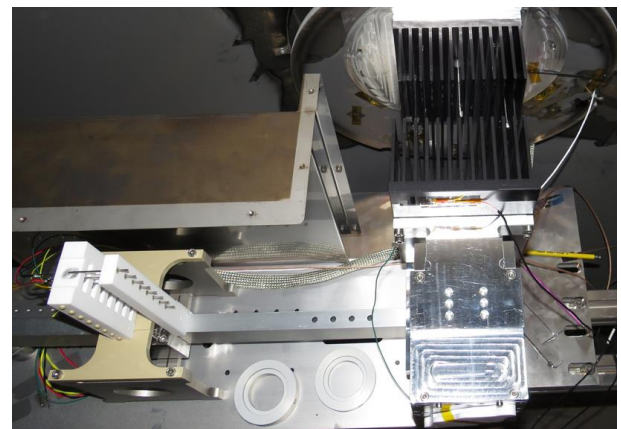


Figure 4. The NANO R<sup>3</sup> mounted onto the thrust balance in FOTEC's vacuum facility

In order to dump the dissipated heat of the integrated PPU of the micro-propulsion system, a thermal radiation based cooling system was developed which consists of two customized overlapping aluminum heat sinks whereas the lower heat sink in the picture is mounted on the moveable beam of the balance and the upper heat sink is directly mounted on the ALM (Additive Layer Manufacturing) aluminum thermal interface plate which is actively cooled

externally by the use of a chiller which can cool down to -20 °C. This ensures contactless cooling of the NANO R<sup>3</sup> and allows continuous operation at all operation points.

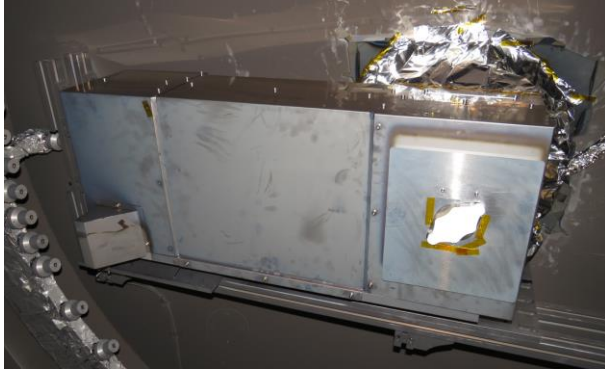


Figure 5. The thrust balance is covered by shields to reduce any chamber effects

To further minimize the effect of back-scattered ions and particles from the chamber walls, special grounded metal shields are used as shown in Figure 5. This also protects the electric feedthroughs from possible leakage currents or spark-overs caused by back sputtering products. The thruster was aligned to allow parallel plasma diagnostic scans in addition to direct thrust measurements. The plasma diagnostic arm equipped with 23 DFCs can be seen in Figure 5 (left, bottom).

Thrust / I <sub>sp</sub> [s]	2,500	3,000	3,500	4,000	4,500
10 μN					X
25 μN					X
50 μN		X	X	X	X
100 μN	X	X	X	X	X
150 μN	X	X	X	X	
200 μN	X	X	X	X	
250 μN	X	X	X		
300 μN	X	X	X		
350 μN		X	X		
400 μN		X			

Table 3. Operation points used for the qualification of the NANO R<sup>3</sup> micro-propulsion module

Different thrust levels between 10 and 400 μN at different specific impulse levels ranging from 2,500 to 4,500 s were tested in this campaign. All operation points are listed in Table 3.

During the test, the operation points were automatically commanded by a script. Each thrust level was

applied for 160 seconds followed by a pause of the same duration during which no thrust was applied. All 28 operation points were tested in the same way.

## 6 THRUST COMPUTATION

The thrust generated by a FEEP-based propulsion system can be computed as

$$T = I_{em} \cdot \sqrt{\frac{2 \cdot m \cdot V_{em}}{q_e}} \cdot f$$

with the emitter current  $I_{em}$ , the mass of an indium ion  $m$ , the emitter voltage  $V_{em}$ , the elementary charge  $q_e$  and the so-called thrust coefficient  $f$ . It could be demonstrated that numeric simulations based on this equation match very accurately with FOTEC's advanced high precision plasma diagnostic measurements with in-house developed DFCs (Digital Faraday Cups) [20]–[22].

The thrust coefficient mainly takes into account the cosine losses due to the beam divergence. Simulations and experiments have shown that at very negative extractor potential, a beam widening occurs that increases the beam divergence angle and consequently reduces the  $f$  factor. Details can be found in [21], Figure 15. Due to the space charge effect (the mutual repulsion of emitted ions), an increasing beam divergence with increasing emitter current is predicted by simulations and could also be verified experimentally. Details can be found in [20], Figure 14.

For the calibration measurements, the firmware used a constant thrust coefficient  $f = 0.8$  so that in most cases the achieved thrust lies above the commanded value and only deviates from this behaviour for extreme operation points.

## 7 CALIBRATION RESULTS

After the thruster was heated up to liquefy the propellant indium, it was ignited. Following the burn-in phase, an impedance characterization was performed, followed by the execution of the test script which commanded all operation points from Table 3. At first the highest specific impulse of 4,500 s was commanded, and the different thrust levels were applied. Then the specific impulse was decreased in accordance with Table 3. The data

gathered from the thrust balance are shown in Figure 6. A moving-average filter was applied to reduce the noise of the readings.

Due to the internal limitations of the PPU (emitter voltage is limited to +10 kV, extractor voltage is limited to -10 kV), the operation points 350  $\mu\text{N}$  / 3,500 s, 350  $\mu\text{N}$  / 3,000 s and 400  $\mu\text{N}$  / 3,000 s could not be reached due to the high impedance of the crown emitter selected for this test campaign. During production, a preselection of crown emitters is performed to allow reaching specific operation points, if requested by the customer. The thrust points 200, 250 and 300  $\mu\text{N}$  at the specific impulse of 3,000 s were not stable as visible in the chart. This was caused by the test firmware of the PPU where the optimization of the PID controllers has not yet been done.

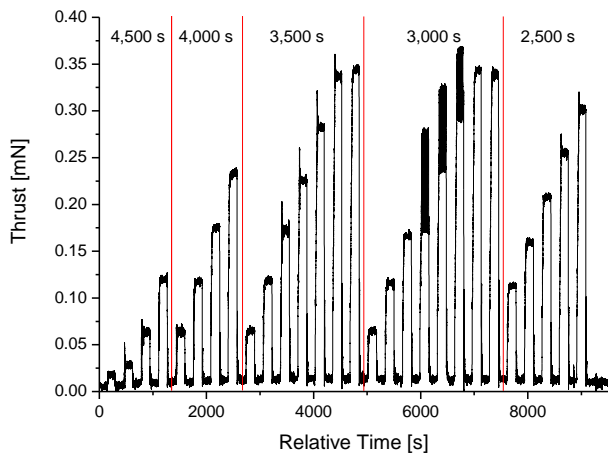


Figure 6. Raw measurement data of all applied operation points

When no thrust is applied, one can recognize that the measured thrust does not return to zero, but a certain offset remains ( $< 13 \mu\text{N}$ ). This was caused by non-thermal equilibrium caused by thruster operation. The offset error was considered and subtracted for the following data analysis. For the measurement of one operation point the change in offset is negligible.

The uncertainty of the force actuators is the main contribution to the total error budget of the thrust balance. Calibration of both force actuators before this campaign yielded relative errors of 0.4 and 0.8%. Therefore, the  $2\sigma$  uncertainty of 2% was used for all measurements.

In Figure 7 the absolute deviation between the measured and commanded thrust is shown whereas the operation points that were not reached are not visible. Disregarding these points, the max. deviation is 23  $\mu\text{N}$  for the operation point 300  $\mu\text{N}$  / 3,500 s.

In Figure 8 the relative deviation between the measured and commanded thrust is shown whereas the operation points that were not reached are omitted again. Disregarding these points and the thrust points below 50  $\mu\text{N}$ , the relative deviation is max. 10% for operation point 200  $\mu\text{N}$  / 4,000 s.

## 8 DATA ANALYSIS

Data analysis has shown good correlation between the model-based thrust computation done by the firmware and the direct thrust measurement. Nevertheless, it could also be shown that at some operation points at very negative extractor voltage or high emitter current, the beam divergence increases which results in a lower thrust coefficient and thus in a lower thrust generated.

The gathered data allowed to optimize the firmware by taking the prevailing effect into account and to compute an extractor voltage dependent thrust coefficient

$$f \rightarrow f(V_{ex})$$

This leads to the more accurate computation of the thrust of a FEFP-based propulsion system

$$T = I_{em} \cdot \sqrt{\frac{2 \cdot m \cdot V_{em}}{q_e}} \cdot f(V_{ex})$$

The updated thrust formula was applied to the acquired operation points and the absolute deviation between the corrected and commanded thrust is shown in Figure 9. The deviation could significantly be reduced, and the max. difference is 9  $\mu\text{N}$  for the operation point 250  $\mu\text{N}$  / 3,000 s. Again, the operation points, that could not be met, were omitted.

In Figure 10 the relative deviation between the corrected and commanded thrust is shown. Disregarding the excluded operation points from Figure 8 and the thrust points below 50  $\mu\text{N}$ , the relative deviation is max. 5.4% for operation point 50  $\mu\text{N}$  / 3,500 s.

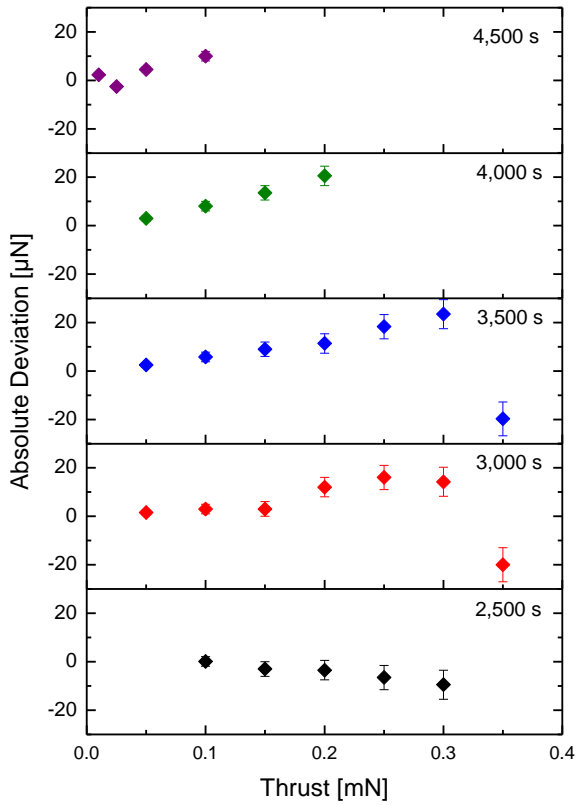


Figure 7. Absolute deviation between measured and commanded thrust

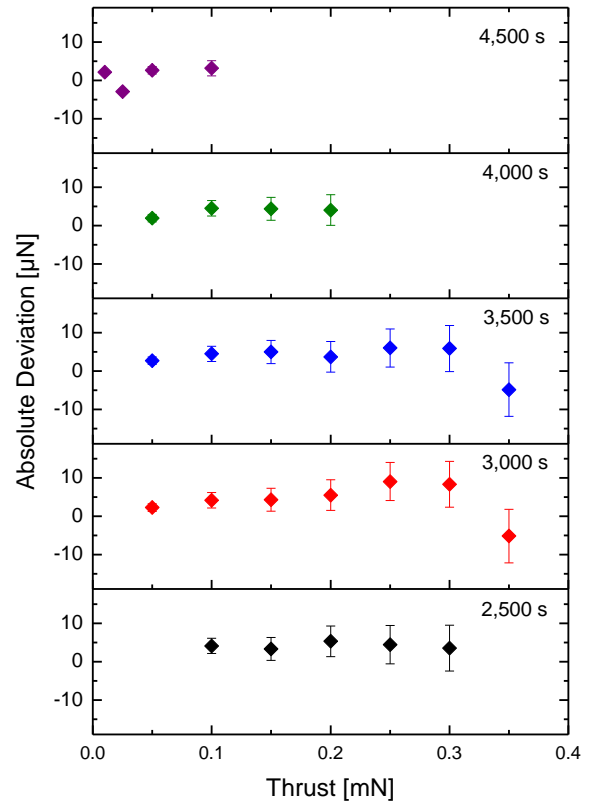


Figure 9. Absolute deviation between corrected and commanded thrust

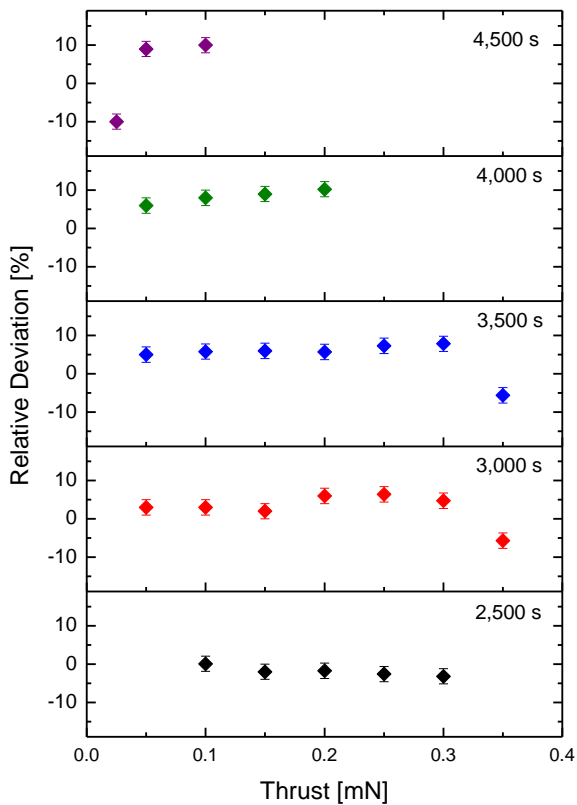


Figure 8. Relative deviation between measured and commanded thrust

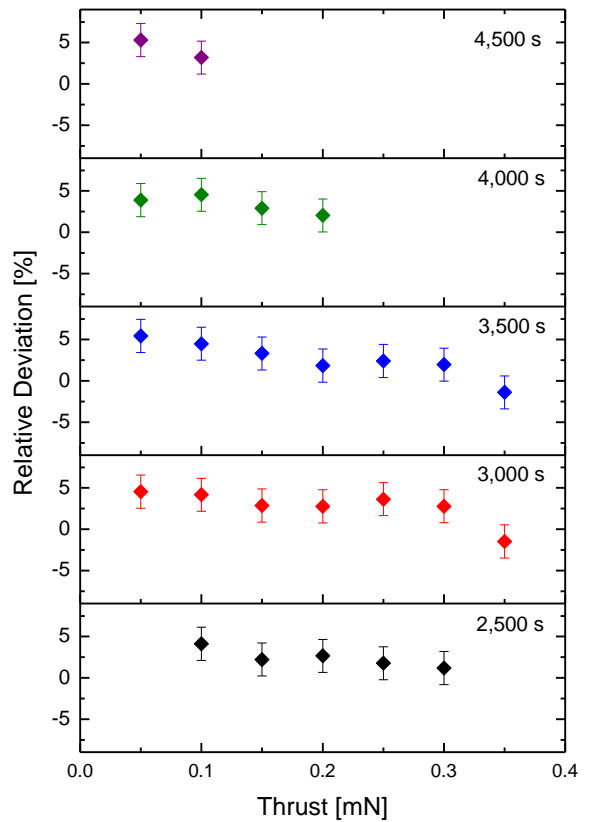


Figure 10. Relative deviation between corrected and commanded thrust

## 9 CONCLUSIONS

In the presented test campaign, the thrust generated by an ENPULSION NANO R<sup>3</sup> micro-propulsion system was directly measured on FOTEC's sub- $\mu$ N to 1 N thrust balance. This paper shows the correlation between the thrust computed by the firmware based on internal telemetry and direct thrust measurements for different operation points (thrust and specific impulse).

A calibration run with a constant thrust coefficient was used to characterize the dependency of the thrust coefficient on the extractor voltage. This allowed to establish a more detailed thrust model for a large operation envelope. It could be shown that the deviation between the measured and the commanded thrust could be significantly reduced by the use of the updated thrust model which is now implemented in the NANO R<sup>3</sup> firmware by default.

## 10 ACKNOWLEDGEMENTS

The research on Indium FEEP technology was strongly supported by the Austrian Research Promotion Agency (FFG) and ESA. The porous Tungsten crown emitter, in particular, was developed within a multitude of projects in the framework of ESA's TRP and EOEP programs.

The development of the NANO R<sup>3</sup> and the direct thrust measurement campaign were supported by project "Qualification of the IFM Thruster Family", Contract Number 4000127313/19/I-DT under the ESA InCubed program framework.

## REFERENCES

- [1] D. Krejci *et al.*, "ENPULSION NANO and MICRO propulsion systems: development and testing," 2021.
- [2] I. Vasiljevich *et al.*, "Development of an Indium mN-FEEP Thruster," Jul. 2008. doi: 10.2514/6.2008-4534.
- [3] B. Seifert, A. Reissner, and T. Hörbe, "Computer Architecture of the PPU for Integrated FEEP Propulsion System," presented at the ARCS 2017 - 30th International Conference on Architecture of Computing Systems, 2017.
- [4] B. Seifert, A. Reissner, N. Buldrini, F. Plesescu, and C. Scharlemann, "Development and Verification of a  $\mu$ N Thrust Balance for High Voltage Electric Propulsion Systems," presented at the 33rd International Electric Propulsion Conference, Washington, D.C., Oct. 2013. Accessed: Jul. 16, 2014. [Online]. Available: [http://erps.spacegrant.org/uploads/images/images/iepc\\_articledownload\\_1988-2007/2013index/vvs6dqil.pdf](http://erps.spacegrant.org/uploads/images/images/iepc_articledownload_1988-2007/2013index/vvs6dqil.pdf)
- [5] N. S. Mühlich, J. Gerger, B. Seifert, and F. Aumayr, "Simultaneously measured direct and indirect thrust of a FEEP thruster using novel thrust balance and beam diagnostics," *Submitted to Acta Astronaut.*
- [6] B. Seifert *et al.*, "Verification of the FOTEC mu-N Thrust Balance at the ESA Propulsion Lab," presented at the Joint Conference of 30th International Symposium on Space Technology and Science 34th International Electric Propulsion Conference and 6th Nanosatellite Symposium, Hyogo-Kobe, Japan, Jul. 2015.
- [7] L. Bettiol, B. Seifert, N. S. Mühlich, L. Masotti, and J. Gonzalez del Amo, "Development and Qualification of the FEEP Technology for the upcoming ESA's Earth Observation Mission NGGM," presented at the 72nd International Astronautical Congress, 2021.
- [8] A. Reissner, N. Buldrini, B. Seifert, F. Plesescu, C. Scharlemann, and J. G. del Amo, "mN-FEEP Thruster Module Design and Preliminary Performance Testing," presented at the 33rd International Electric Propulsion Conference, Washington, D.C., USA, Oct. 2013. Accessed: Jul. 16, 2014. [Online]. Available: [http://erps.spacegrant.org/uploads/images/images/iepc\\_articledownload\\_1988-2007/2013index/c1r8ixn1.pdf](http://erps.spacegrant.org/uploads/images/images/iepc_articledownload_1988-2007/2013index/c1r8ixn1.pdf)
- [9] A. Reissner, N. Buldrini, B. Seifert, and F. Plesescu, "Detailed Performance Characterization of the mN-FEEP Thruster," presented at the Space Propulsion 2014, Cologne, Germany, May 2014. [Online]. Available: [www.propulsion2014.com](http://www.propulsion2014.com)
- [10] I. Vasiljevich, N. Buldrini, F. Plesescu, M. Tajmar, M. Betto, and J. Gonzalez del Amo, "Porous tungsten crown multiemitter testing programme using three different grain sizes and sintering procedures," presented at the 32nd International Electric Propulsion Conference, Wiesbaden, Germany, Sep. 2011. Accessed: Jul. 16, 2014. [Online]. Available: [http://erps.spacegrant.org/uploads/images/images/iepc\\_articledownload\\_1988-2007/2011index/IEPC-2011-065.pdf](http://erps.spacegrant.org/uploads/images/images/iepc_articledownload_1988-2007/2011index/IEPC-2011-065.pdf)

- [11] I. Vasiljevich, N. Buldrini, F. Plesescu, M. Tajmar, M. Betto, and J. del Amo, "Consolidation of milli-Newton FEEP Thruster Technology based on Porous Tungsten Multiemitters," Jul. 2011. doi: 10.2514/6.2011-5592.
- [12] M. Tajmar, I. Vasiljevich, and W. Grienauer, "High current liquid metal ion source using porous tungsten multiemitters," *Ultramicroscopy*, vol. 111, no. 1, pp. 1–4, Dec. 2010, doi: 10.1016/j.ultramic.2010.09.005.
- [13] M. Tajmar *et al.*, "Development of a porous tungsten mN FEEP thruster," presented at the Space Propulsion Conference 2010, San Sebastian, 2010.
- [14] B. Seifert, A. Reissner, D. Jelem, and T. Hörbe, "Development of a Low Cost PPU for FEEP Electric Propulsion using COTS Components," presented at the 11th European Space Power Conference - ESPC 2016, Thessaloniki, Greece, Sep. 2016.
- [15] D. Jelem, B. Seifert, R. Sypniewski, N. Buldrini, and A. Reissner, "Performance Mapping and Qualification of the IFM Nano Thruster FM for in Orbit Demonstration," Jul. 2017. doi: 10.2514/6.2017-4887.
- [16] B. Seifert *et al.*, "In-Orbit Demonstration of the Indium-Feep IFM Nano Thruster," presented at the 6th Space Propulsion Conference, Sevilla, Spain, May 2018.
- [17] ENPULSION, "ENPULSION NANO R3." 2019. Accessed: Mar. 26, 2022. [Online]. Available: <https://www.enpulsion.com/wp-content/uploads/ENP2019-086.E-ENPULSION-NANO-R3-Product-Overview.pdf>
- [18] K. Marhold and M. Tajmar, "Micronewton Thrust Balance for Indium FEEP Thrusters," Jul. 2005. doi: 10.2514/6.2005-4387.
- [19] N. Buldrini, M. Tajmar, K. Marhold, and B. Seifert, "Experimental Results of the Woodward Effect on a  $\mu$ N Thrust Balance," Jul. 2006. doi: 10.2514/6.2006-4911.
- [20] N. S. Mühlich, B. Seifert, and F. Aumayr, "Verification of simulation model based on beam diagnostics measurements of the IFM Nano Thruster," presented at the 72nd International Astronautical Congress (IAC), Oct. 2021.
- [21] N. S. Mühlich, B. Seifert, and F. Aumayr, "IFM Nano Thruster performance studied by experiments and numerical simulations," *J. Phys. Appl. Phys.*, Nov. 2020, doi: 10.1088/1361-6463/abc84c.
- [22] N. S. Mühlich, B. Seifert, E. Ceribas, J. Gerger, and F. Aumayr, "High-Precision Digital Faraday Cups for FEEP Thrusters," presented at the 72nd International Astronautical Congress (IAC), Dubai, Oct. 2021.